Non-aggregated Intercalation of Dicationic Tetraphenylporphyrinatoantimony(V) Complexes into Smectite Clay Layers

Tsutomu Shiragami,* Keiko Nabeshima, Jin Matsumoto, Masahide Yasuda, and Haruo Inoue[†]
Department of Applied Chemistry, Faculty of Engineering, Miyazaki University, Gakuen-Kibanadai, Miyazaki 889-2192
[†]*CREST, JST (Japan Science and Technology)*

(Received February 14, 2003; CL-030127)

Adsorption and intercalation of +2 charged cationic [3-(trimethylammonio)propoxo(methoxo)(tetraphenylporphyrinato)-antimony(V)]$^{2+}$ (**1a**) into an artificially synthesized smectite clay were studied. The red shift of Soret band in UV-spectra for **1a** in an aqueous colloidal clay solution and analyses of X-ray diffraction of the obtained complex between **1a** and the clay indicate the intercalation of **1a** into the clay interlayer. Ammonium cationic part on an axial ligand led to the effective non-aggregated intercalation of **1a** into the clay.

Intercalation of some functional molecules into multi-layered inorganic materials such as clays has been extensively studied from the interesting as providing nanospace chemical reaction sites.[1,2] Several studies on the interaction between porphyrin and cation exchangeable clays have recently reported from the viewpoints of unique photochemical reaction in nanospace interlayer.[3,4] In these clay systems, the aggregation of porphyrin molecules was often observed,[2] and caused a disadvantage for a photoreaction owing to decrease of the excited state lifetime. Therefore, the control of aggregation is necessary to make photoreaction effective in the clay system. Recently, we have reported that the intercalation of new type of cationic dihydroxo(porphyrinato)antimony(V) complex into an artificially synthesized cation-exchangeable smectite clay (Sumecton SA; SSA) was effectively induced. Although the structure of their axial ligands was an important factor for providing a complete intercalated porphyrin-SSA complex, axial hydroxo ligand did not prevent the aggregation in SSA interlayer[5] If the distance and orientation of porphyrin ring in interlayer of anionic SSA sheets can be controlled by the introduction of cationic axial ligand, it will be expected to prevent the aggregation of porphyrin in SSA interlayers. Here, we report on the adsorption and intercalation behaviors of novel 3-trimethylammoniopropoxo- and 3-dimethylaminopropoxo-(methoxo)(tetraphenylporphyrinato)antimony(V) complexes (**1a**, **b**)[6] into SSA, as shown in Figure 1.

The measurement of absorption spectra was performed for a solution prepared by mixing the aqueous solution of **1a**, **b** (5.0×10^{-6} mol dm^{-3}) with colloidal SSA solution (50 mg dm^{-3}).[5] The loading level of **1a**, **b** vs cationic exchange capacity of SSA (%LL) were adjusted by the addition of variable amounts of SSA to constant concentration of **1a**, **b**. Figure 2 shows the absorption spectra of **1a**, **b** under the conditions of various %LL in aqueous colloidal SSA solution. At low %LL (10–20%), the λ_{max} of Soret band of **1a** (418 nm) and **1b** (419 nm) was shifted to a longer wavelength (431 nm). In the case of **1b**, an increase of %LL led the further red shift of λ_{max} and the broading of Soret band. Similar spectral change was observed in hydroxo axial ligand system.[5] These spectral changes clearly demonstrated the adsorption and aggregation of **1b** onto the surface or in the interlayer space of SSA[7] However, the absorption spectra of **1a** did not show the larger red shift and further broading of Soret band with an increase of %LL, suggesting that the π–π interaction between porphyrin rings each other should be weaker in **1a**-SSA system. **1a**, **b** were adsorbed onto SSA quantitatively, since no absorption peaks of **1a**, **b** were detected in their filtrates by the filtration of **1**-SSA powders whereas free **1a**, **b** were observed in the aqueous SSA colloidal solution at a 120%LL.

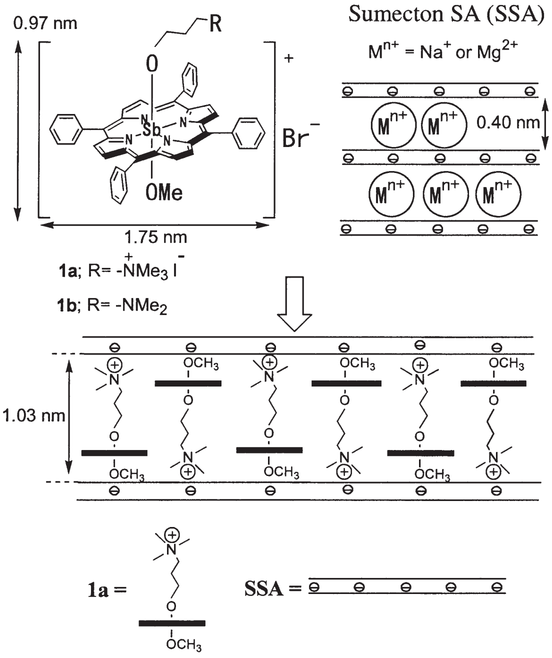

Figure 1. Schematic diagram of possible layered structure.

X-ray diffraction (XRD) analysis was performed for the samples prepared by filtration of the above mixture through a membrane filter (pore size = 1 µm) and drying at room temperature. In the case of **1a**-SSA complex, some broad diffraction peaks were observed on XRD measurement, indicating that the layer structure of SSA should be kept irrespective of the addition of **1a** (Figure 3A). As an increase of %LL, the interlayer distance of **1a**-SSA complex increased to reach 1.03 nm in 100 %LL, as shown in Figure 3B. According to PM3 calculation, the thickness of **1a** for axial ligand direction was estimated to be ca. 0.94 nm. This value is almost consistent with the interlayer distance (1.03 nm) of **1a**-SSA complex. These results strongly suggest that **1a** should be intercalated into SSA inter-

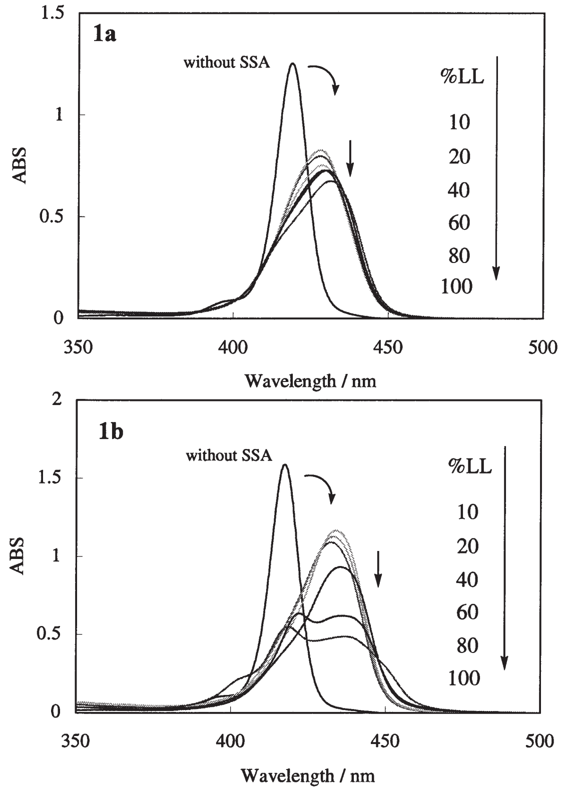

Figure 2. Absorption spectra of **1a** and **1b** at various %LL for aqueous **SSA** solution.

layer space at a high %LL, and that the orientation of the porphyrin plane should be almost parallel to the SSA clay layer, as shown in Figure 1. If the orientation of **1a** is vertical to the clay layer, the expanded interlayer distance should be about 1.75 nm. On the other hand, XRD measurements for **1b**-SSA complex gave no diffraction peaks, indicating that SSA should become amorphous by the addition of **1b**, as shown in previous report.[5] Accordingly, these results show that **1b**-SSA complex can not take the layer structure but adsorbed and aggregated on SSA surface.

Thus, it is clear that the ammonium cationic group as an axial ligand was effective not only for the intercalation into SSA, but for non-aggregation of porphyrin. The axial cationic part gave the fine intercalated structure where the porphyrin rings could be located with the alternate orientation (head-to-tail) probably owing to the strong Coulombic attractive force with anionic clay sheets, resulting that non-aggregation of **1a** can be achieved in SSA interlayer. This is a first example for the intercalation of dicationic porphyrin system having both axial ligand part and porphyrin part into the clay layer. The above results show the importance of the axial ligand structure as to how to control the aggregation of porphyrins in interlayer space of clay.

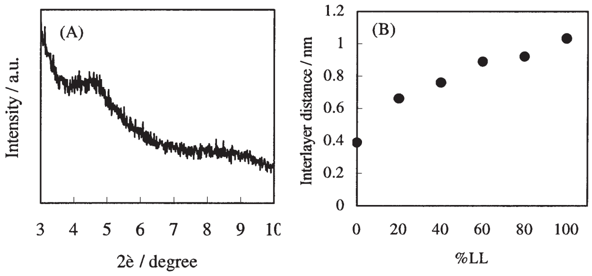

Figure 3. (A) The XRD profile of **1a-SSA** at %LL = 80%. (B) Relationship between the %LL and the interlayer distance determined by XRD measurement of **1a-SSA**.

This research was supported by a Grand-in-Aid for Scientific Research (No. 14050079. Scientific Research in Priority Areas 417) from the Ministry of Education, Science, Sports, and Culture. We are grateful to Mr. Kukizaki and Ms. Akazaki (Miyazaki Prefecture Industrial Technology Center) for XRD measurement.

References and Notes

1 J. K. Thomas, *Chem. Rev.*, **93**, 301 (1993).

2 a) K. Takagi and T. Shichi, "Solid State and Surface Photochemistry," ed. by V. Ramamurthy and K. S. Schanze, Marcel Dekker, New York (2000), Vol. 5, p 31. b) M. Ogawa and K. Kuroda, *Chem. Rev.*, **95**, 399 (1995).

3 a) H. Kaneyama, H. Suzuki, and A. Amano, *Chem. Lett.*, **1988**, 1117. b) I. Y. Park, K. Kuroda, and C. Kato, *Chem. Lett.*, **1989**, 2057. c) K. A. Carrado and R. E. Winans, *Chem. Mater.*, **2**, 328 (1990). d) I. Ukrainczyk, M. Chibwe, T. J. Pinnavaia, and S. A. Boyd, *J. Phys. Chem.*, **98**, 2668 (1994). e) M. Onaka, T. Shinoda, K. Aichi, K. Suzuki, and Y. Izumi, *Mol. Cryst. Liq. Cryst.*, **277**, 149 (1996). f) Z. Chernia and D. Gill, *Langmuir*, **6**, 1350 (1999). g) S. Bonnet, C. Forano, A. De Roy, and J. P. Besse, *Chem. Mater.*, **8**, 1965 (1996).

4 a) S. Takagi, T. Shimada, M. Eguchi, T. Yui, H. Yoshida, D. A. Tryk, and H. Inoue, *Langmuir*, **18**, 2265 (2002). b) Z. Tong, T. Shichi, K. Oshika, and K. Takagi, *Chem. Lett.*, **2002**, 876. c) S. Takagi, D. A. Tryk, and H. Inoue, *J. Phys. Chem. B*, **106**, 5455 (2002).

5 T. Shiragami, K. Nabeshima, M. Yasuda, and H. Inoue, *Chem. Lett.*, **2003**, 148.

6 Preparation of **1a**, **b**: Mono-methanolysis of dibromo(tetraphenylporphyrinato)antimony(V) ($[Sb(tpp)Br_2]^+Br^-$) was performed in MeOH–MeCN (1:1) to give $[Sb(tpp)(Br)(OMe)]^+Br^-$.[8] An MeCN–pyridine solution (5:1 v/v 50 mL) containing $[Sb(tpp)(Br)(OMe)]^+Br^-$ (1.1 mmol) and *N*,*N*-dimethyl-3-amino-1-propanol (30 mmol) was heated for 2 h at 65 °C. The solvent was evaporated and then solved in CH_2Cl_2. The CH_2Cl_2 solution was washed three times with 50 mL portions of H_2O. After evaporation, the crude product was chromatographed on SiO_2 using $CHCl_3$–MeOH (10:1, v/v) as an eluent to give **1b**. MeI (32 mmol) was added in an MeCN–pyridine solution (5:1 v/v 50 mL) containing **1b** and then heated for 2 h at 65 °C for methylation of dimethyl amino group. The purification of **1a** was performed by same procedure with **1b**. **1b**: Yield 80%; UV-vis (MeOH) λ_{max}/nm (log ε): 419 (5.58), 551 (4.25), and 591 (4.09); SIMS: *m/z* 866 (M^+-2H); ^1H NMR ($CDCl_3$/ppm) δ −2.65 (2H, t, $J =$ 6.2 Hz $-OCH_2-$), −2.29 (3H, s, $-OCH_3$), −1.58 (2H, quint, $J = 6.2$ Hz, $-CH_2-$), −0.20 (2H, t, $J = 6.2$ Hz, $-CH_2-N-$), 1.40 (6H, s, $-N(CH_3)_2$), 7.79–7.93 (12H, m, Ph), 8.23 (4H, d, $J =$ 6.7 Hz, Ph), 8.34 (4H, d, $J = 6.7$ Hz, Ph), 9.48 (8H, s, pyrrole). **1a**: Yield 94% from **1b**; UV-vis (MeOH) λ_{max}/nm (log ε): 419 (5.48), 551 (4.15), and 591 (3.93); SIMS: m/z 881 (M^+-2H); ^1H NMR ($CDCl_3$/ppm) δ −2.59 (2H, t, $J = 6.0$ Hz, $-OCH_2-$), −2.24 (3H, s, $-OCH_3$), −1.14 (2H, quint, $J = 6.0$ Hz, $-CH_2-$), 0.89 (2H, t, $J = 6.0$ Hz, $-CH_2-^+N-$), 2.18 (9H, s, $-^+N(CH_3)_3$), 7.83–8.00 (12H, m, Ph), 8.24 (4H, d, $J = 6.6$ Hz, Ph), 8.67 (4H, d, $J = 6.6$ Hz, Ph), 9.58 (8H, s, pyrrole).

7 M. Kasha, H. R. Rawls, and M. A. El-Bayoumi, *Pure Appl. Chem.*, **11**, 371 (1965).

8 T. Shiragami, Y. Andou, Y. Hamasuna, F. Yamaguchi, K. Shima, and M. Yasuda, *Bull. Chem. Soc. Jpn.*, **75**, 1577 (2002).

Published on the web (Advance View) May 6, 2003; DOI 10.1246/cl.2003.484